

# Coalescence, genetic diversity and sexual populations under selection

Richard A. Neher<sup>1</sup>, Taylor A. Kessinger<sup>1</sup> and Boris I. Shraiman<sup>2,3</sup>

<sup>1</sup>Max Planck Institute for Developmental Biology, 72076 Tübingen, Germany, <sup>2</sup> Kavli Institute for Theoretical Physics, and

<sup>3</sup>Department of Physics, University of California, Santa Barbara, 93116, CA, USA

(Dated: February 7, 2022)

In sexual populations, selection operates neither on the whole genome, which is repeatedly taken apart and re-assembled by recombination, nor on individual alleles that are tightly linked to the chromosomal neighborhood. The resulting interference between linked alleles reduces the efficiency of selection and distorts patterns of genetic diversity. Inference of evolutionary history from diversity shaped by linked selection requires an understanding of these patterns. Here, we present a simple but powerful scaling analysis identifying the unit of selection as the genomic “linkage block” with a characteristic length,  $\xi_b$ , determined in a self-consistent manner by the condition that the rate of recombination within the block is comparable to the fitness differences between different alleles of the block. We find that an asexual model with the strength of selection tuned to that of the linkage block provides an excellent description of genetic diversity and the site frequency spectra when compared to computer simulations. This linkage block approximation is accurate for the entire spectrum of strength of selection and is particularly powerful in scenarios with many weakly selected loci. The latter limit allows us to characterize coalescence, genetic diversity, and the speed of adaptation in the infinitesimal model of quantitative genetics.

In asexual populations, different genomes compete for survival, and the fate of most new mutations depends more on the total fitness of the genome they reside in than on their own contribution to fitness. As a result, beneficial mutations on one genetic background can be lost to competition with other backgrounds, an effect known as “clonal interference” (Desai and Fisher, 2007; Gerrish and Lenski, 1998; Neher, 2013), and likewise deleterious mutations in very fit genomes can fix. This interference is reduced by recombination and disappears when recombination is rapid enough such that selection can act independently on different loci. Many eukaryotes recombine their genetic material by crossing over of homologous chromosomes. As a result, distant loci evolve independently, but nearby tightly linked loci remain coupled. Such interference, known as Hill-Robertson interference, reduces the efficacy of selection (Barton, 1995; Hill and Robertson, 1966) and reduces levels of neutral variation. Neutral diversity is indeed correlated with local recombination rates in several species, suggesting that linked selection is an important evolutionary force (Begun and Aquadro, 1992; Cutter, 2006). One typically distinguishes background selection against deleterious mutations (Charlesworth *et al.*, 1993; Hudson and Kaplan, 1995) from sweeping beneficial mutations, which lead to hitch-hiking (Gillespie, 2000; Maynard Smith and Haigh, 1974). Both of these processes reduce diversity at linked loci and probably contribute to the observed correlation (Hudson, 1994). Another piece of evidence for the importance of linked selection comes from the weak correlation between levels of genetic diversity and the population size (Lefler *et al.*, 2012). Whereas classic neutral models predict that diversity should increase linearly with the population size (Kingman, 1982), in models dominated by selection the diversity depends only weakly on the population size (Neher, 2013). Hence linked selection could explain this “paradox of variation” (Lewontin, 1974).

From the perspective of a neutral allele, any random association with genetic backgrounds of different fitness results in fluctuations of its allele frequency. To distinguish this

source of stochasticity from genetic drift, Gillespie coined the term “genetic draft” (Gillespie, 2000). While genetic draft is well understood when caused by strongly selected mutations whose dynamics is deterministic at high frequencies (Barton, 1995; Walczak *et al.*, 2012; Weissman and Barton, 2012), the cumulative effect of many weak effect mutations has mainly been addressed using simulations (Gordo *et al.*, 2002a; McVean and Charlesworth, 2000). Many populations harbor substantial heritable phenotypic variation which in an unknown way depends on a large number of polymorphisms in the genome. The majority of these polymorphisms are likely to have small effects on phenotypes and fitness. Collectively, however, they still can dominate phenotypic variation (Yang *et al.*, 2010) and possibly fitness variation. This limit is known as the infinitesimal model in quantitative genetics. Quantitative genetics, however, typically ignores linkage between loci and the maintenance of genetic diversity (Bulmer, 1980; Lynch and Walsh, 1998).

Here, we characterize the structure of genealogies, genetic diversity and the rate of adaptation in sexual populations in the limit of numerous weakly selected alleles. We build on recent progress in our understanding of genealogies in adapting asexual populations (Brunet *et al.*, 2007; Desai *et al.*, 2013; Neher and Hallatschek, 2013) and we will first review these results briefly. We will then present a scaling argument that reduces the problem of coalescence within an sexually reproducing population to an asexual population with suitably scaled parameters. This correspondence allows us to predict levels of genetic diversity, coalescence time scales, and site frequency spectra. Our results hold regardless of whether the polymorphisms originated as weakly deleterious or beneficial mutations and thus cover weak effect background selection or adaptation. We confirm the validity of the mapping to the asexual model by comparing its predictions with numerical simulations of evolving sexual populations. We use this approximation to demonstrate that in the limit of numerous weakly selected mutations, the rate of adaptation scales as the square root of recombination rate.

## I. RESULTS

In asexual populations all loci share the same genealogical history, and the fate of a lineage depends on the fitness of the entire genome. If fitness depends on a large number of polymorphic loci with comparable effects, the fitness distribution in the population will be roughly Gaussian, and the fittest individuals are  $x_c \approx \sigma\sqrt{2\log N\sigma}$  ahead of the fitness mean, where  $\sigma^2$  is the total fitness variance in the population (Desai and Fisher, 2007; Rouzine *et al.*, 2003; Tsimring *et al.*, 1996). In large asexual populations, only individuals in the high fitness nose have an appreciable chance to contribute to future generations. It will take those individuals roughly  $\sigma^{-1}\sqrt{2\log N\sigma}$  generations to dominate the population. Hence the probability that two randomly chosen individuals had a common ancestor  $\sigma^{-1}\sqrt{2\log N\sigma}$  generations ago is of order one, i.e., their ancestral lineages have likely coalesced. A more thorough analysis of coalescence in adapting asexual populations can be found in Refs. (Desai *et al.*, 2013; Neher and Hallatschek, 2013)<sup>1</sup>. In small populations with  $N\sigma \ll 1$ , coalescence is dominated by neutral processes (non-heritable fluctuations in offspring number known as genetic drift). The average number of generations back to the most recent common ancestor of any pair of extant genomes, a.k.a. the pair coalescence time, is given by:

$$\langle T_2 \rangle \approx \begin{cases} N & N\sigma \ll 1 \\ c\sigma^{-1}\sqrt{2\log N\sigma} & N\sigma \gg 1 \end{cases} \quad (1)$$

where  $c$  is a constant of order one that captures deviations from Gaussianity that depend on details of the model. For the infinitesimal model studied here  $c = \sqrt{12}$ .

In an attempt to extend applicability of the neutral coalescent, one sometimes defines an “effective population size”,  $N_e$ , equal to  $\langle T_2 \rangle$  regardless of whether coalescence is neutral or not (Charlesworth, 2009). By definition a neutral model with  $N_e = \langle T_2 \rangle$  predicts the same levels of genetic diversity, but the statistical properties of the genealogies dominated by selection are quite different and cannot be papered over simply by redefining the population size. We will therefore avoid the term  $N_e$  and stick to  $\langle T_2 \rangle$ . For the approximately neutral case,  $N\sigma \ll 1$ , the coalescent tree is of the Kingman type (Kingman, 1982). As  $N\sigma$  increases, coalescence is more and more driven by the amplification of fit genomes, which generates a very skewed offspring number distribution over timescales of order  $\sigma^{-1}$ . As a result, the genealogies resemble the Bolthausen-Sznitman coalescent (BSC) (Bolthausen and Sznitman, 1998; Brunet *et al.*, 2007) with very different statistical properties. Two representative coalescent trees sampled from asexual populations, one neutral and one rapidly adapting, are shown in Fig. 1A.

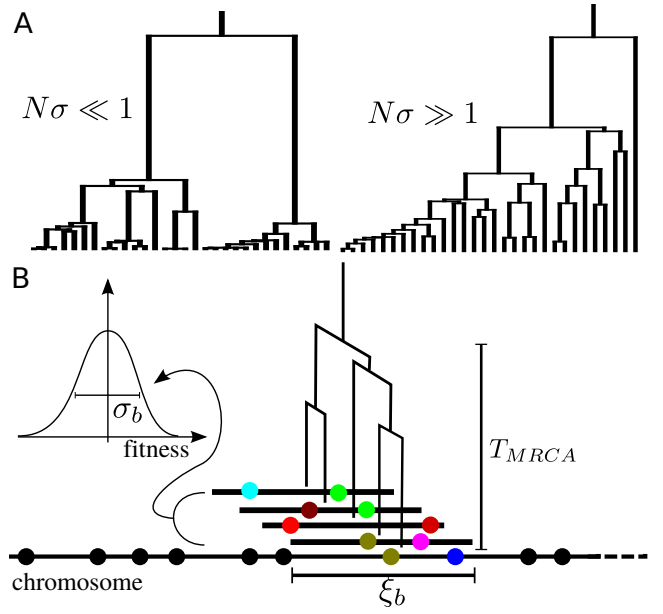


Figure 1 Coalescence in neutral and adapting populations. Panel (A) shows a typical coalescent tree from neutral and adapting asexual populations (left and right, respectively). In adapting populations, coalescent trees branch asymmetrically and contain approximate multiple mergers. Panel (B) illustrates asexual blocks in sexual populations. The sketch depicts a representative chromosome at the bottom with polymorphisms indicated as balls. Different loci within segments shorter than  $\xi_b$  share most of their genealogical history, i.e., have trees similar to the one indicated in the center of the segment. Coalescence within this segment of length  $\xi_b$  is either neutral or driven by the fitness differences between different haplotypes spanning these segments. The fitness distribution of these haplotype blocks is indicated as inset. Distant parts of the chromosome are in linkage equilibrium, and the tree changes as one moves along the chromosome. The succession of changing trees is the ancestral recombination graph.

### Sexual populations and recombination.

In contrast to asexual evolution, recombination decouples different loci in sexual populations – the further apart, the more rapidly. The typical length of the segment that is not interrupted over a time  $t$  along one ancestral lineage decreases with time as

$$\xi = \frac{L}{1 + L\rho t} \approx \frac{1}{\rho t} \quad (2)$$

where  $\rho$  is the crossover rate and  $L$  is the length of the chromosome. The second approximation is justified whenever  $\xi \ll L$ . If polymorphisms affecting fitness are spread evenly across the genome and are dense (the infinitesimal model), we expect that different segregating haplotypes in a region of length  $\xi(t)$  harbor fitness variation proportional to the segment length

$$\sigma_\xi^2 = \frac{\xi(t)}{L} \sigma^2. \quad (3)$$

This fitness variance shrinks with time as the block length decreases. While initial fitness differences between blocks are

<sup>1</sup> In Ref. (Neher and Hallatschek, 2013) it is shown that  $\langle T_2 \rangle \approx \sigma^2/D$ . Since  $\sigma^2 \approx (24D^2 \log N\sigma)^{1/3}$ ,  $\langle T_2 \rangle \approx c\sigma^{-1}\sqrt{2\log N\sigma}$  with a  $c = \sqrt{12}$ .

large, they are chopped into smaller blocks so rapidly that selection has no time to amplify the fittest of these early large blocks. But the rate at which blocks are chopped up decreases as they get shorter, and at some point the rate of chopping them up is outweighed by the amplification of the fittest blocks by selection. The latter happens when fitness differences between haplotypes of this block are comparable to the recombination rate. More precisely, the relevant block length  $\xi(t)$  is the length that survives over the time scale of coalescence, i.e.,  $\xi_b = \xi(\langle T_2 \rangle)$ . In large enough populations, the time scale of coalescence itself is determined by these fitness differences via Eq. 1. In contrast to asexual populations, only the fitness variance,  $\sigma_b^2$ , within the linkage block of length  $\xi_b$  is relevant rather than the total variance  $\sigma^2$  (see illustration in Fig. 1B). Using  $\langle T_2 \rangle = c\sigma_b^{-1}\sqrt{2\log N\sigma_b}$  in Eq. 2, we find for the length of linked blocks

$$\xi_b = \frac{\sigma_b}{c\rho\sqrt{2\log N\sigma_b}}. \quad (4)$$

LD measured in populations samples should decay over this length scale. Substituting  $\xi_b$  into Eq. 3 yields

$$\sigma_b = \frac{\sigma^2}{L\rho c\sqrt{2\log N\sigma_b}} \quad \text{and} \quad \xi_b = \frac{\sigma^2}{2L\rho^2 c\log N\sigma_b}. \quad (5)$$

Hence the time scale of coalescence and neutral diversity are given by the inverse of the fitness variance per map length  $R = L\rho$  with a logarithmic correction (see also (Hudson and Kaplan, 1995; Santiago and Caballero, 1998) for the case of strongly selected mutations). To arrive at this result, we have assumed that coalescence is driven by selection, i.e., we have assumed  $N\sigma_b \gg 1$ . If this condition is not satisfied, local coalescence will be approximately neutral. In this case  $\langle T_2 \rangle = N$  and the LD extends over  $\xi_b \sim (N\rho)^{-1}$  nucleotides. Empirically, we observe a smooth and rapid crossover between these two regimes (see below and Fig. 2).

The condition for draft dominance,  $N\sigma_b \gg 1$ , is more stringent in sexual populations than in asexual populations, in which it is  $N\sigma \gg 1$ . In other words, recombination reduces interference and results in drift dominated coalescence over a larger parameter range. We predict now that the results for genetic diversity in the asexual coalescent apply with  $\sigma_b^2$  as the local fitness variance and that linkage disequilibrium between common loci extends over a distance  $\xi_b$ . We will validate these predictions by forward simulations of different population models.

#### Constant selection in the infinitesimal model.

We first consider a model of a population whose fitness variance is set by external (environmental) factors in which the selected trait depends on many weak effect polymorphisms and de novo mutations; see Model and Methods. This model might be a first approximation to scenarios where selection pressures are dictated by a changing environment, an evolving immune system, or a breeder who imposes a constant artificial selection. We simulate our population using

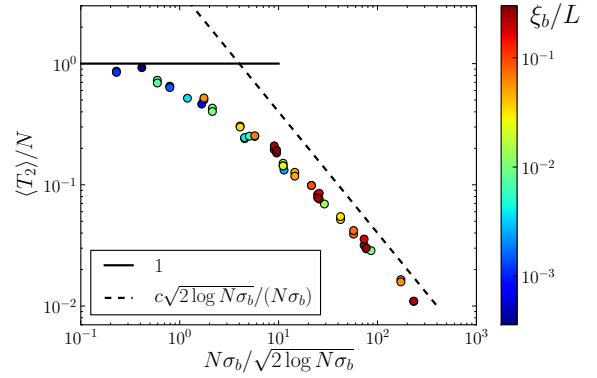


Figure 2 Coalescence in sexual populations. The figure shows the average pair coalescence time  $\langle T_2 \rangle$  relative to the neutral expectation as a function of  $N\sigma_b$  determined using Eq. 5. For  $N\sigma_b \ll 1$ ,  $\langle T_2 \rangle \approx N$ , while  $\langle T_2 \rangle = c\sigma_b^{-1}\sqrt{2\log N\sigma_b}$  otherwise.

a discrete generation model with an approximately constant population size and a finite number of sites in the genome as implemented in FFPopSim (Zanini and Neher, 2012) (see Methods). We track the genealogy of a locus in the center of the chromosome, which allows us to study properties of representative coalescent trees.

After allowing the population to equilibrate, we sample the evolving population in roughly  $\langle T_2 \rangle$  intervals and measure  $T_2$ ,  $T_{MRCA}$ , the site frequency spectrum (SFS), and the linkage disequilibrium (LD) between polymorphisms at intermediate frequencies ( $[0.1, 0.9]$ ). We perform these simulations for many combinations of parameters. For each of these combinations, we calculate  $\sigma_b$  according to Eq. 5. Fig. 2 shows that the average pair coalescence time  $\langle T_2 \rangle$  approaches  $N$  for  $N\sigma_b \rightarrow 0$  and that it is proportional to  $\sigma_b^{-1}$  (with logarithmic corrections) for  $N\sigma_b \gg 1$  as predicted.

In addition to a reduction in genetic diversity, we predict that the local genealogies will resemble samples from the BSC rather than the Kingman coalescent whenever  $N\sigma_b \gg 1$ . Fig. 3 shows a collection of SFS colored by the  $N\sigma_b$ . With increasing  $N\sigma_b$ , the SFS smoothly interpolate between the expectations for the Kingman coalescent and the BSC. As soon as the SFS starts deviating from the prediction of the Kingman coalescent, Tajima's D and related measures turn negative. For large  $N\sigma_b$ , we find a non-monotonic SFS with a steep divergence  $f(v) \sim v^{-2}$  for rare alleles characteristic of the BSC.

Another important feature of diversity in sexual populations is the genomic distance across which loci share much of their genealogy. This can be quantified by measuring the correlations between loci (LD) at different distances. In order for our picture to be consistent, the extent of LD should be approximately equal to  $\xi_b = (\rho\langle T_2 \rangle)^{-1}$ . We measured LD as  $r^2(d)$  for different distances  $d$  and plot its distance dependence against  $d/\xi_b$ ; see Fig. 4. As predicted, the distance over which loci are correlated is well described by  $\xi_b = (\rho\langle T_2 \rangle)^{-1}$ .

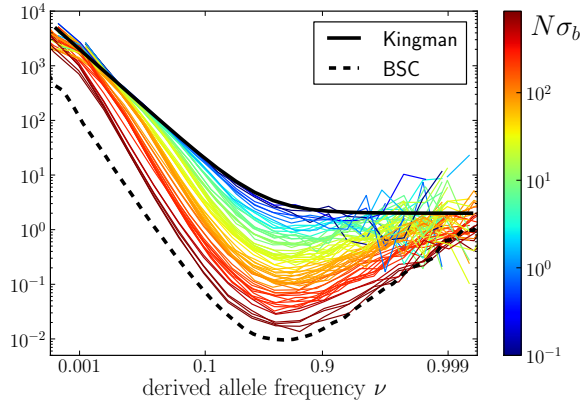


Figure 3 Site frequency spectra (SFS). The figure shows the SFS, normalized by  $\Theta = 2N\mu$ , for a large number of parameter combinations. Color indicates the value of  $N\sigma_b$ . For large  $N\sigma_b$ , the SFS display the non-monotonicity characteristic of the BSC (dashed line), while the SFS are well described by the prediction from Kingman's coalescent (solid line) if  $N\sigma_b \ll 1$ . The BSC curve serves as a guide to the eye since its normalization depends on  $N\sigma_b$ .

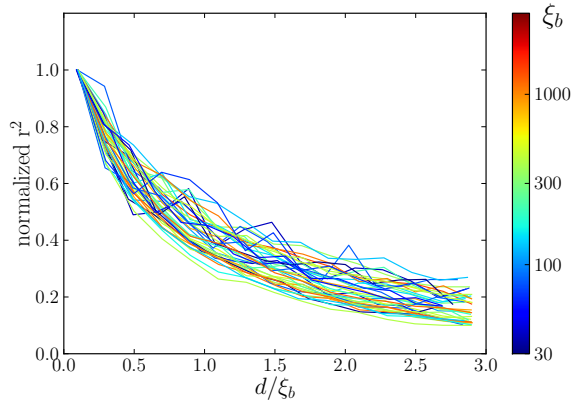


Figure 4 Correlation length along the genome. The figure shows linkage disequilibrium, quantified as average  $r^2$ , between pairs of loci at different distances (the curves are normalized to their value at zero distance). The x-axis shows the distance between loci  $d$  rescaled by  $\xi_b$  determined using Eq. 2 with  $t$  equal to the measured pair coalescence time. After this rescaling, the distance dependence of all simulations follow approximately the same master curve, which shows that LD extends for  $\approx \xi_b$ .

#### Frequent small effect mutations.

In the model studied above, fitness variance was set by external factors. We now consider a model where the fitness variance and diversity are set by a balance between frequent novel mutations of small effect and the removal of variation by selection, i.e., fixation or loss of alleles. This type of model has been studied for asexual populations (Cohen *et al.*, 2005a; Tsimring *et al.*, 1996). Using these results, we expect that the

fitness variance within a block of length  $\xi_b$  is given by

$$\sigma_b^2 \approx \frac{\xi_b \mu \langle s^2 \rangle}{2} \langle T_2 \rangle. \quad (6)$$

Here,  $\mu$  is the mutation rate, and  $\langle s^2 \rangle$  is the second moment of the distribution of mutational effects. Note that in this infinitesimal limit it is irrelevant whether mutations are deleterious or beneficial – only the second moment of the fitness effect distribution is important. The quantity  $D = \frac{\xi_b \mu \langle s^2 \rangle}{2}$  is the “diffusion” constant of haplotype fitness in the absence of selection. Eq. 6 implies that fitness variation accumulates over the time it takes a few lineages to dominate the population, which is approximately given by the half the pair coalescence time (Neher and Hallatschek, 2013). Substituting Eq. 2 with  $t = \langle T_2 \rangle$  into Eq. 6, we find

$$\sigma_b^2 = \frac{\mu \langle s^2 \rangle}{2\rho} \quad (7)$$

Remarkably, this variance of the effectively asexual blocks is simply the ratio of variance injection per nucleotide,  $\mu \langle s^2 \rangle$ , and the crossover rate (at least while  $N\sigma_b \gg 1$ ). The coalescence time cancels! We therefore find for  $\langle T_2 \rangle$

$$\langle T_2 \rangle \approx \begin{cases} N & N\sqrt{\mu \langle s^2 \rangle \rho^{-1}} \ll 1 \\ c\sqrt{\frac{\rho \log N\sigma_b}{\mu \langle s^2 \rangle}} & N\sqrt{\mu \langle s^2 \rangle \rho^{-1}} \gg 1 \end{cases} \quad (8)$$

where  $c$  is again a constant of order 1. In the limit where coalescence is driven by selection, the total rate of adaptation is therefore

$$\sigma^2 \approx cL\sqrt{\rho \mu \langle s^2 \rangle \log N\sigma_b}. \quad (9)$$

These results apply to steadily adapting populations (i.e. scenarios where beneficial mutations dominate), populations suffering from a mutational meltdown, or populations where the two processes balance. We simulate the lattermost using a model with recurrent mutations such that the population settles into a dynamic equilibrium where the fixation of beneficial mutations is roughly canceled out by that of deleterious mutations (Goyal *et al.*, 2012). The predictions for neutral diversity, LD and the SFS match the simulation results very well. Supplementary figure S1 shows plots analogous to Fig. 2 through 4. The prediction for the total fitness variance, Eq. 9, is compared to the simulation results in Fig. 5. We investigated additional models to demonstrate the robustness of the conclusions regarding model assumptions and simulation method. Supplementary figure S2 shows neutral diversity, LD, and SFS for a model in which unique beneficial mutations are injected at sites that become monomorphic. Supplementary figure S3 shows results for a bona fide infinite sites model of chromosomes of length 1 that undergo one crossover per generation and accumulate beneficial or deleterious mutations at rate  $U$ . In all of these cases, the observed diversity agrees well with the predictions of Eq. 8 and the SFS show the expected crossover from the Kingman to the BSC predictions as  $N\sigma_b$  increases.



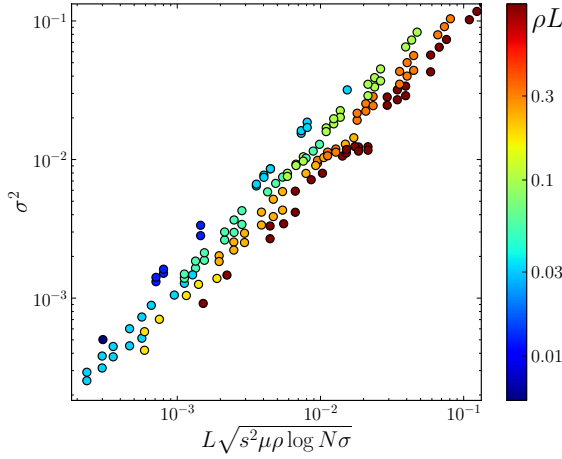


Figure 5 The total fitness variation due to frequent weak effect mutations in a model where deleterious and beneficial mutations balance each other. The color shows the average number of crossovers per simulated segment. There is a residual dependence on  $\rho$  due to large corrections to the asymptotic behavior.

#### Loosely linked loci.

Our analysis has focused on the effect of fitness variation in short effectively asexual blocks. As discussed above, the total strength of selection  $\sigma$  can be much larger than the fitness differences within effectively asexual blocks  $\sigma_b$ . However, a particular locus only remains linked to distant polymorphisms for a short time, and the contribution of these distant loci averages out. For our focus on the effect of tightly linked loci to be valid, the integral contribution of such loosely linked loci to drift and draft should be small compared to the effect of fitness variation  $\sigma_b$  within the segment. Loosely linked loci are amenable to a perturbative analysis known as Quasi-Linkage Equilibrium (Kimura, 1965; Neher and Shraiman, 2011a). In Ref. (Neher and Shraiman, 2011a) it is shown that the stochastic dynamics of the allele frequency  $v_i$  at locus  $i$  due to loosely linked loci is described by the following Langevin equation:

$$\frac{d}{dt}v_i(t) = v_i(1 - v_i)s_i + 2\mu(1 - 2v_i) + \sum_{i \neq j} D_{ij}(t)s_j + \eta_i(t), \quad (10)$$

where  $D_{ij}(t)$  is the LD between loci  $i$  and  $j$ ,  $s_j$  is the fitness effect of the derived allele at locus  $j$ , and  $\eta_i$  is random noise with autocorrelation function  $\langle \eta_i(t)\eta_i(t') \rangle = N^{-1}\delta(t - t')$ , representing genetic drift. If the two loci are loosely linked, i.e., the crossover rate  $c_{ij}$  between them is much larger than the effect of selection on either of them,  $D_{ij}$  is also a fluctuating quantity. The autocorrelation function of  $D_{ij}$  is (Neher and Shraiman, 2011a)

$$\langle D_{ij}(t)D_{ij}(t') \rangle = \frac{v_i(1 - v_i)v_j(1 - v_j)e^{-c_{ij}|t - t'|}}{2Nc_{ij}}. \quad (11)$$

Given this autocorrelation, we can now integrate over fluctuations due to genetic drift and loosely linked selected loci to

obtain a renormalized diffusion coefficient, i.e., the reduction of the “effective population size”. Reproducing Eq. 44 of (Neher and Shraiman, 2011a), we have

$$\frac{N}{N_e} = 1 + \frac{1}{2} \sum_{i \neq j} v_j(1 - v_j) \frac{s_j^2}{c_{ij}^2} \quad (12)$$

This result is similar to results in (Hudson and Kaplan, 1995; Nordborg *et al.*, 1996; Santiago and Caballero, 1998) in that it shows that the level of drift is increased by a factor that depends on the square of the ratio of selection and linkage, averaged over the genome.

If we now consider the integral effect of all loci further away than  $\xi$ , it is always dominated by the loci at the smallest distance, so that  $N/N_e - 1 \sim (\sigma/R)^2(\xi/L)^{-1}$  (obtained as a continuum approximation to the sum in Eq. 12,  $R = \rho L$ ). Hence, provided that  $\xi/L > (\sigma/R)^2$  – a condition that obtains when fitness variation at distant loci is sufficiently small or the loci are sufficiently distant – their effect can be accounted for by a simple rescaling of the effective population size (Weissman and Barton, 2012); this is the *weak draft* regime. Note, however, that the recombination rate between distant loci is ultimately limited by the outcrossing rate and that distant loci can have substantial effects in facultatively sexual populations (Neher *et al.*, 2010; Weissman and Barton, 2012).

The negligible effect of loosely linked loci is a consequence of two types of averaging that are apparent in Eq. 11: (i) The associations between these distant loci are transient and average out over time. This manifests itself in the decay time of  $c_{ij}^{-1}$  in Eq. 11. (ii) Different individuals carry different alleles at these distant loci, and hence their fitness effect is averaged over different descendents. As a consequence, the autocorrelation in Eq. 11 is proportional to  $(Nc_{ij})^{-1}$ . Together, these two averages result in the  $1/c_{ij}^2$  contribution of loosely linked loci.

For the more tightly linked loci, i.e.,  $\xi < \xi_* = (\sigma/R)^2 L$ , the behavior crosses over to the *strong draft* regime. This crossover length scale  $\xi_*$  is controlled entirely by the *local* quantities: the recombination rate per base pair  $\rho$  and the local fitness variance density. Furthermore,  $\xi_*$  is in general larger than  $\xi_b$ , with  $\xi_*/\xi_b \sim \log(N\sigma_b)$ . This ratio corresponds to the reduction in the block size during the span of time between local selection effects first coming into play and the coalescence time. In the limit of  $\log(N\sigma_b) \gg 1$  recombination events within the  $\xi_*$  block must be reckoned with, but for more realistic population sizes, we have shown above that focusing on the  $\xi_b$ -sized asexual segment captures the effects of strong draft quite well.

#### Length distribution of segments identical by descent (IBD).

The structure of genealogies has implications for the length  $\ell$  of IBD segments in pairs of individuals. Their distribution,  $p(\ell)$ , is directly related to the distribution of pair coalescence times,  $q(T_2)$ , via the relation  $p(\ell) \sim \int dT_2 q(T_2) e^{-\rho \ell T_2}$ . In neutrally evolving populations of constant size, pair coalescence times are exponentially distributed with mean  $\langle T_2 \rangle = N$ .

Consequently, the length of IBD segments is distributed as  $p(\ell) \sim 1/(1 + \rho\ell\langle T_2 \rangle)$  and has a long slowly decaying tail. If  $N\sigma_b \gg 1$ , coalescence is accelerated on average but predominantly happens after lineages have reached the upper tail of the fitness distribution of different alleles of a linkage block. Hence the distribution of pair coalescence times is peaked at  $\langle T_2 \rangle$  rather than being exponential; comp. Fig. 3 in ref. (Neher and Hallatschek, 2013). This shift in the distribution of  $T_2$  with relatively rare very recent coalescence has the consequence that  $p(\ell) \sim e^{-\rho\ell\langle T_2 \rangle}$  is approximately exponential. Long IBD segments are therefore much less likely than in the neutral case with the same  $\langle T_2 \rangle$ .

## II. DISCUSSION

In most sexual populations, the histories of different chromosomes or loci far apart on a chromosome are weakly correlated. Nearby loci, however, are more tightly linked, which results in correlated histories and linkage disequilibrium. Since the density of heterozygous sites is  $\pi = 2\mu\langle T_2 \rangle$  and the length scale of LD is  $\xi_b = (\rho\langle T_2 \rangle)^{-1}$ , the typical number of SNPs in one linkage block is  $n \approx \mu/\rho$ . If  $n$  is much larger than one, and a sizeable fraction of those SNPs affect fitness, different haplotypes segregating within such a block will display a broad distribution in local fitness with a variance that we have denoted by  $\sigma_b^2$ . Neutral alleles linked to haplotypes drawn from this distribution will be affected by linked selection. This in turn results in genealogies different from standard neutral models but similar to the Bolthausen-Sznitman coalescent (BSC) characteristic of rapidly adapting asexual populations (Neher and Hallatschek, 2013; Neher and Shraiman, 2011b).

In regions of high recombination in obligately outcrossing species the number of polymorphisms per linkage block,  $n$ , is of order one and linked selection will mainly result from the occasional strong selective sweep (Sella *et al.*, 2009). But recombination rates vary by orders of magnitude across the genome (Comeron *et al.*, 2012) and  $n \gg 1$  in low recombination regions. In those regions, the cumulative effect of many weakly selected polymorphisms is expected to be important. This holds in particular for species that outcross rarely, such as many plants, nematodes, yeasts, and viruses (Barrière and Félix, 2005; Bomblies *et al.*, 2010; Neher and Leitner, 2010; Tsai *et al.*, 2008). This type of linked selection will overwhelm genetic drift if  $N\sigma_b > 1$ . The fitness variance per block is given by  $\sigma_b^2 = \langle s^2 \rangle \pi \xi_b$ , where  $\langle s^2 \rangle$  is the second moment of the effect distribution of polymorphisms. Hence we require  $N^2 \langle s^2 \rangle > (\pi \xi_b)^{-1} = n^{-1}$ . Provided  $n$  is large enough, even nominally neutral ( $Ns < 1$ ) polymorphisms collectively dominate the dynamics of haplotypes of length  $\xi_b$ . In this infinitesimal limit, the nature of linked selection is irrelevant and our results apply to any mix of deleterious and beneficial mutations as long as the effects of individual mutations are weak and their number is large.

## Relation to previous work.

Most previous work on genetic draft and selective interference considered mutations with strong effects that behave deterministically at high frequencies, whereas we focus on weak effect mutations. Reduction of genetic diversity by sweeping beneficial mutations was first discussed by Maynard Smith (Maynard Smith and Haigh, 1974); see also (Barton, 1998; Braverman *et al.*, 1995; Gillespie, 2000; Kaplan *et al.*, 1989). In these models, genetic diversity is determined by the typical waiting time between two successive selective sweeps close enough to affect a given locus. Similarly, deleterious mutations reduce diversity at linked sites. Assuming that mutations have a large detrimental effect on fitness and happen with rate  $\mu$  per site, it was shown in refs. (Hudson and Kaplan, 1995; Nordborg *et al.*, 1996) that the reduction of genetic diversity is a function of  $\mu/\rho$ . As in our analysis here, the strongest effect on genetic diversity comes from tightly linked loci. Our analysis of loosely linked loci is similar to the work by Santiago and Caballero (Santiago and Caballero, 1998). The latter, however, breaks down at tight linkage, and the crossover to the asexual behavior is essential for a consistent description in the limit of many weakly selected loci. This limit has mainly been studied using computer simulations (Gordo *et al.*, 2002b; McVean and Charlesworth, 2000; Messer and Petrov, 2013), and few analytical results are available.

Weissman and Barton (Weissman and Barton, 2012) investigated the rate of adaptation and its effect on diversity using scaling arguments similar to the one presented here. In their model, adaptation is driven by individual selective sweeps. The duration of a sweep explicitly sets the time scale  $\langle T_2 \rangle$  on which coalescence happens. In this model, the speed of adaptation is proportional to the map length. In contrast, our model assumes many weak effect mutations, and the time scale of coalescence is set by  $\sigma_b$ , which is self-consistently determined and itself depends on model parameters such as  $\rho$  and  $\mu\langle s^2 \rangle$ . We can recover their result for the rate of adaptation by setting  $\langle T_2 \rangle \sim s^{-1}$  and  $\xi_b \sim s/\rho$ . With these assumptions, we obtain

$$\sigma^2 \sim L\rho s \quad (13)$$

instead of Eq. 9. The model used in Ref. (Weissman and Barton, 2012) applies to a limit where at most one strongly selected and sweeping mutation falls into one linkage block, but our analysis considers the opposite limit. The basic properties of genealogies and SFS are expected to be qualitatively similar in the limit of one sweep per block. If the contribution from weak mutations is negligible while sweeps are common, the coalescence properties will be dominated by sweeps at different distances. This limit has been studied in (Durrett and Schweinsberg, 2005) and also results in a multi-merger coalescent.

Other types of models are appropriate if the rate of outcrossing is small compared to the standard deviation in fitness (Neher and Shraiman, 2011b; Neher *et al.*, 2010; Rouzine and Coffin, 2005) or if recombination proceeds via horizontal transfer of short pieces of DNA (Cohen *et al.*, 2005b; Neher *et al.*, 2010). In these cases, one finds a very strong dependence of the rate of adaptation on the rate of outcrossing or

horizontal transfer. Rare recombination has the potential to dramatically increase fitness variance because many loci are in strong LD.

In summary, we have characterized the effect of dense weakly selected polymorphisms on genetic diversity, which might be the source of much of the phenotypic variability we observe (Lynch and Walsh, 1998; Yang *et al.*, 2010). Our analysis provides a consistent genealogical framework for the infinitesimal model of quantitative genetics. This limit of weakly selected mutations has so far eluded analytical understanding. We derived equations that relate the mutational input and the rate of recombination to neutral diversity and the site frequency spectra. Because genetic diversity (neutral or not) is directly accessible in population resequencing experiments, our results should be of practical relevance when interpreting such data. Furthermore, one is often interested in identifying particular mutations that arose in response to specific environmental challenges. If successful, those mutations tend to be of large effect and fall outside the scope of our model. Importantly, strong adaptations only perturb a fraction of the genome (more precisely a segment of length  $\approx s(\rho \log Ns)^{-1}$ , where  $s$  is the selection coefficient). Our model provides the background on top of which such singular adaptations can be sought, and understanding the statistical patterns of diversity and linkage within this null model is essential for reliable inference.

### III. ACKNOWLEDGEMENTS

We would like to thank Fabio Zanini for stimulating discussions and help with FFPopSim and Guy Sella for very useful comments on the manuscript. This work is supported by the ERC starting grant HIVEVO 260686 to R.A.N and in part by the NSF PHY11-25915 grant to KITP. B.I.S. acknowledges support from NIH R01 GM086793.

### IV. METHODS

We use a model with discrete generations, haploid individuals, an approximately constant population size, and a finite number of sites in the genome, as implemented in FFPopSim (Zanini and Neher, 2012). We simulate a fraction of a chromosome of length  $L$ , where outcrossing happens with rate  $\rho$  between randomly chosen gametes and results in a single crossover. If  $\rho L \ll 1$ , no recombination happens in most cases. In addition to forward simulation, we also track the genealogy of a central locus, which allows us to measure pair coalescence times, the time to the MRCA, and the neutral SFS directly (this functionality is implemented in a more recent release of FFPopSim; see <http://code.google.com/p/ffpopsim>). For all parameters, we produce equilibrated populations by simulating for  $10 T_{MRCA}$ . Subsequent measurements of population parameters start from these equilibrated populations and sample the population roughly twice every  $\langle T_2 \rangle$  as estimated from our theoretical arguments. All scripts associated with this paper can be obtained from

<http://git.tuebingen.mpg.de/reccoal>.

#### A. Constant selection

To maintain a constant fitness variance  $\sigma^2$ , we rescale the selection coefficients associated with individual loci each generation accordingly. Mutations are introduced into a random individual whenever a locus becomes monomorphic, i.e., the previously introduced mutation is lost or has fixed (see (Neher and Shraiman, 2011b)). This allows us to simulate a large number of sites efficiently in a limit where the overall mutation rate is small compared to  $\langle T_2 \rangle$ . In this way, we keep all  $L$  loci polymorphic without employing a high mutation rate, which would result in frequent recurrent mutations. We simulate a grid of parameters with  $N$  taking the values [1000, 3000, 10000],  $\sigma$  the values [0.01, 0.03, 0.1], and  $L\rho$  five logarithmically spaced values between  $0.1\sigma$  and  $1.0\sigma$ . For the analysis, simulations were filtered so that  $\xi_b > 30$  and  $\xi_b < L/3$ . To prevent invalid logarithms,  $\log(N\sigma_b)$  was replaced by  $\log(N\sigma_b + 2)$  in Eq. 5.

#### B. Dynamic Balance

In this set of simulations, we simulate a genome consisting of finite sites in a constant fitness landscape where mutations at each locus have a small effect  $s$ . Mutations are injected at random with rate  $\mu$  at each locus. In contrast to the models above, where mutations are injected only when a locus is monomorphic, we allow recurrent and back mutation to make the dynamic balance state possible. The grid of parameters used was  $L \in [3000, 10000]$ ,  $N \in [1000, 3000, 10000]$ ,  $s \in [-0.001, -0.003, -0.01]$ ,  $L\mu \in [1, 3, 10, 30]$ , and  $L\rho$  logarithmically spaced between  $s$  and  $1.0$ . For the analysis, simulations were filtered such that  $\xi_b > 30$ ,  $\xi_b < L/3$ , and  $\langle T_2 \rangle \mu < 0.5$ .

### References

- Barrière, A., and M.-A. Félix, 2005, *Current Biology* **15**(13), 1176, ISSN 0960-9822, URL <http://www.sciencedirect.com/science/article/pii/S096098220500655X>.
- Barton, N., 1998, *Genet Res* **72**(02), 123, URL <http://journals.cambridge.org/action/displayAbstract?aid=3537>.
- Barton, N. H., 1995, *Genetics* **140**(2), 821, URL <http://www.genetics.org/cgi/reprint/140/2/821>.
- Begun, D. J., and C. F. Aquadro, 1992, *Nature* **356**(6369), 519, URL <http://www.nature.com/doifinder/10.1038/356519a0>.
- Bolthausen, E., and A.-S. Sznitman, 1998, *COMMUNICATIONS IN MATHEMATICAL PHYSICS* **197**(2), 247.
- Bomblies, K., L. Yant, R. A. Laitinen, S.-T. Kim, J. D. Hollister, N. Warthmann, J. Fitz, and D. Weigel, 2010, *PLoS Genet* **6**(3), e1000890, URL <http://dx.doi.org/10.1371/journal.pgen.1000890>.
- Braverman, J. M., R. R. Hudson, N. L. Kaplan, C. H. Langley, and W. Stephan, 1995, *Genetics* **140**(2), 783, URL <http://www.genetics.org/cgi/reprint/140/2/783>.

- Brunet, E., B. Derrida, A. H. Mueller, and S. Munier, 2007, Physical review E, Statistical, nonlinear, and soft matter physics **76**(4 Pt 1), 041104, URL <http://scitation.aip.org/getabs/servlet/GetabsServlet?prog=normal&id=PLEEE8000076000004041104000001&idtype=cvips&gifs=yes>.
- Bulmer, M. G., 1980, *The Mathematical Theory of Quantitative Genetics* (Oxford University Press, Oxford).
- Charlesworth, B., 2009, Nat Rev Genet **10**(3), 195, URL <http://www.nature.com/nrg/journal/v10/n3/abs/nrg2526.html>.
- Charlesworth, B., M. T. Morgan, and D. Charlesworth, 1993, Genetics **134**(4), 1289, URL <http://www.genetics.org/cgi/reprint/134/4/1289>.
- Cohen, E., D. A. Kessler, and H. Levine, 2005a, Phys Rev E Stat Nonlin Soft Matter Phys **72**(6 Pt 2), 066126, URL <http://pre.aps.org/abstract/PRE/v72/i6/e066126>.
- Cohen, E., D. A. Kessler, and H. Levine, 2005b, Phys Rev Lett **94**(9), 098102, URL <http://scitation.aip.org/getabs/servlet/GetabsServlet?prog=normal&id=PRLTA000094000009098102000001&idtype=cvips&gifs=yes>.
- Comeron, J. M., R. Ratnappan, and S. Bailin, 2012, PLoS Genet **8**(10), e1002905, URL <http://dx.doi.org/10.1371/journal.pgen.1002905>.
- Cutter, A. D., 2006, Genetics **172**(1), 171, ISSN 0016-6731, 1943-2631, PMID: 16272415, URL <http://www.genetics.org/content/172/1/171>.
- Desai, M. M., and D. S. Fisher, 2007, Genetics **176**(3), 1759, URL <http://www.genetics.org/cgi/content/abstract/176/3/1759>.
- Desai, M. M., A. M. Walczak, and D. S. Fisher, 2013, Genetics **193**(2), 565, ISSN 0016-6731, 1943-2631, PMID: 23222656, URL <http://www.genetics.org/content/193/2/565>.
- Durrett, R., and J. Schweinsberg, 2005, Stochastic Process. Appl. **115**(10), 1628, URL <http://www.ams.org/mathscinet/search/publications.html?pg1=MR&sl=MR2165337>.
- Gerrish, P. J., and R. E. Lenski, 1998, Genetica **102-103**(1-6), 127, URL <http://www.springerlink.com/content/np187h5878166310/>.
- Gillespie, J. H., 2000, Genetics **155**(2), 909, URL [www.genetics.org/cgi/content/abstract/155/2/909](http://www.genetics.org/cgi/content/abstract/155/2/909).
- Gordo, I., A. Navarro, and B. Charlesworth, 2002a, Genetics **161**(2), 835, URL <http://www.genetics.org/cgi/content/full/161/2/835>.
- Gordo, I., A. Navarro, and B. Charlesworth, 2002b, Genetics **161**(2), 835, ISSN 0016-6731, 1943-2631, PMID: 12072478, URL <http://www.genetics.org/content/161/2/835>.
- Goyal, S., D. J. Balick, E. R. Jerison, R. A. Neher, B. I. Shraiman, and M. M. Desai, 2012, Genetics **191**, 1309, URL <http://www.genetics.org/content/early/2012/05/30/genetics.112.141291.long>.
- Hill, W. G., and A. Robertson, 1966, Genet Res **8**(3), 269, URL <http://www.ncbi.nlm.nih.gov/pubmed/5980116?dopt=abstract>.
- Hudson, R. R., 1994, Proceedings of the National Academy of Sciences **91**(15), 6815, ISSN 0027-8424, 1091-6490, PMID: 8041702, URL <http://www.pnas.org/content/91/15/6815>.
- Hudson, R. R., and N. L. Kaplan, 1995, Genetics **141**(4), 1605, URL <http://www.genetics.org/cgi/reprint/141/4/1605>.
- Kaplan, N. L., R. R. Hudson, and C. H. Langley, 1989, Genetics **123**(4), 887, URL <http://www.genetics.org/cgi/reprint/123/4/887>.
- Kimura, M., 1965, Genetics **52**(5), 875, URL <http://www.genetics.org/cgi/reprint/52/5/875>.
- Kingman, J., 1982, Journal of Applied Probability **19A**, 27, URL <http://www.jstor.org/stable/3213548>.
- Leffler, E. M., K. Bullaughey, D. R. Matute, W. K. Meyer, L. Séguirel, A. Venkat, P. Andolfatto, and M. Przeworski, 2012, PLoS Biol **10**(9), e1001388, URL <http://dx.doi.org/10.1371/journal.pbio.1001388>.
- Lewontin, R. C., 1974, *The genetic basis of evolutionary change* (Columbia University Press).
- Lynch, M., and B. Walsh, 1998, *Genetics and Analysis of Quantitative Traits* (Sinauer).
- Maynard Smith, J., and J. Haigh, 1974, Genet Res **23**(1), 23, URL [http://www.ncbi.nlm.nih.gov/sites/entrez?Db=pubmed&Cmd=Retrieve&list\\_uids=4407212&dopt=abstractplus](http://www.ncbi.nlm.nih.gov/sites/entrez?Db=pubmed&Cmd=Retrieve&list_uids=4407212&dopt=abstractplus).
- McVean, G. A., and B. Charlesworth, 2000, Genetics **155**(2), 929, URL <http://www.genetics.org/cgi/content/full/155/2/929>.
- Messer, P. W., and D. A. Petrov, 2013, PNAS **110**(21), 8615, ISSN 0027-8424, 1091-6490, PMID: 23650353, URL <http://www.pnas.org/content/110/21/8615>.
- Neher, R., and B. Shraiman, 2011a, Rev. Mod. Phys. **83**(4), 1283, URL [http://rmp.aps.org/abstract/RMP/v83/i4/p1283\\_1](http://rmp.aps.org/abstract/RMP/v83/i4/p1283_1).
- Neher, R. A., 2013, Annual Review of Ecology, Evolution, and Systematics **44**(1), null, URL <http://www.annualreviews.org/doi/abs/10.1146/annurev-ecolsys-110512-135920>.
- Neher, R. A., and O. Hallatschek, 2013, Proceedings of the National Academy of Sciences **110**(2), 437, ISSN 0027-8424, 1091-6490, URL <http://www.pnas.org/content/110/2/437>.
- Neher, R. A., and T. Leitner, 2010, PLoS Comput Biol **6**(1), e1000660, URL <http://www.ploscompbiol.org/article/metrics/info%253Adoi%252F10.1371%252Fjournal.pcbi.1000660>.
- Neher, R. A., and B. I. Shraiman, 2011b, Genetics **188**, 975, URL <http://www.genetics.org/content/early/2011/05/31/genetics.111.128876.abstract>.
- Neher, R. A., B. I. Shraiman, and D. S. Fisher, 2010, Genetics **184**, 467, URL <http://www.genetics.org/cgi/content/full/184/2/467>.
- Nordborg, M., B. Charlesworth, and D. Charlesworth, 1996, Genet Res **67**(2), 159, URL <http://www.ncbi.nlm.nih.gov/pubmed/8801188?dopt=abstract>.
- Rouzine, I. M., and J. M. Coffin, 2005, Genetics **170**(1), 7, URL <http://www.genetics.org/cgi/content/full/170/1/7>.
- Rouzine, I. M., J. Wakeley, and J. M. Coffin, 2003, Proc Natl Acad Sci USA **100**(2), 587, URL <http://www.pnas.org/content/100/2/587.long>.
- Santiago, E., and A. Caballero, 1998, Genetics **149**(4), 2105, URL <http://www.genetics.org/cgi/content/full/149/4/2105>.
- Sella, G., D. A. Petrov, M. Przeworski, and P. Andolfatto, 2009, PLoS Genet **5**(6), e1000495, URL <http://www.plosgenetics.org/article/info%253Adoi%252F10.1371%252Fjournal.pgen.1000495>.
- Tsai, I. J., D. Bensasson, A. Burt, and V. Koufopanou, 2008, Proc Natl Acad Sci USA **105**(12), 4957, ISSN 0027-8424, 1091-6490, PMID: 18344325, URL <http://www.pnas.org/content/105/12/4957>.
- Tsimring, L., H. Levine, and D. Kessler, 1996, Phys Rev Lett **76**(23), 4440, URL [http://prola.aps.org/abstract/PRL/v76/i23/p4440\\_1](http://prola.aps.org/abstract/PRL/v76/i23/p4440_1).
- Walczak, A. M., L. E. Nicolaisen, J. B. Plotkin, and M. M. Desai, 2012, Genetics **190**, 753.
- Weissman, D. B., and N. H. Barton, 2012, PLoS Genet **8**(6), e1002740, URL <http://dx.doi.org/10.1371/journal>.



[pgen.1002740](#).

- Yang, J., B. Benyamin, B. P. Mcevoy, S. Gordon, A. K. Henders, D. R. Nyholt, P. A. Madden, A. C. Heath, N. G. Martin, G. W. Montgomery, M. E. Goddard, and P. M. Visscher, 2010, *Nat Genet* **42**(7), 565, URL <http://links.ealart.nature.com/ctt?kn=81&m=35253159&r=MzQ5MjM3NTk2OQS2&b=0&j=NzY2NTA5MDcS1&mt=1&rt=0>.
- Zanini, F., and R. A. Neher, 2012, *Bioinformatics* **28**(24), 3332, ISSN 1367-4803, 1460-2059, URL <http://bioinformatics.oxfordjournals.org/content/28/24/3332>.

Supplementary figure 1: recurrent mutations with weak effects

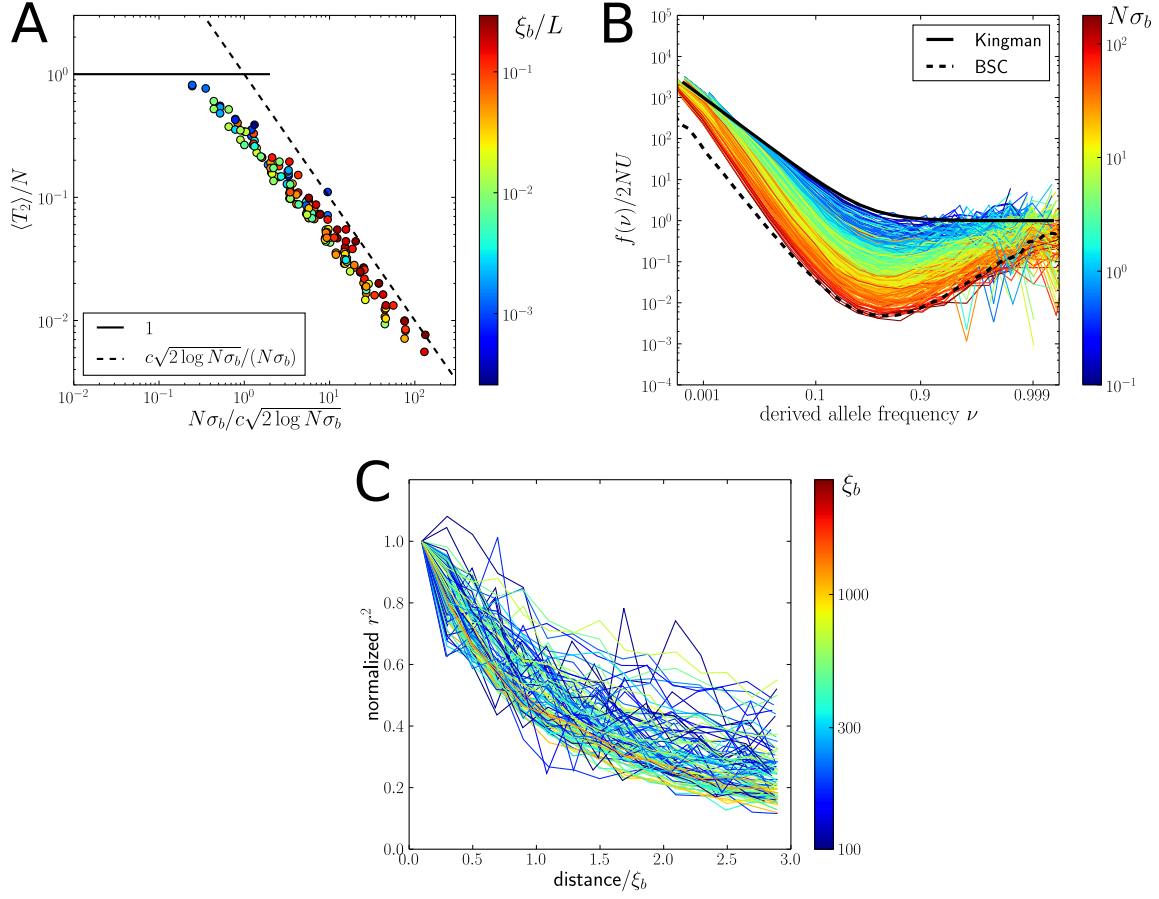


Figure 1 Genetic diversity in populations with recurring mutations between a preferred and unpreferred state with weak effect. Panel A shows the pairwise coalescence time compared to the analytical predictions in the limits of large and small  $N\sigma_b$ . Panel B shows the SFS normalized to  $\Theta = 2N\mu$  (the SFS are obtained from local coalescent trees). Different curves are colored by their respective  $N\sigma_b$  values. The BSC curve serves as a guide to the eye since its proper normalization depends on  $N\sigma_b$ . Panel C shows the decay of LD measured as  $r^2$  and normalized with its value at short distances. The x-axis is rescaled by  $\xi_b$ . The resulting collapse demonstrates that LD extends over distances  $\xi_b$ . The grid of parameters used for simulations was  $L \in [3000, 10000]$ ,  $N \in [1000, 3000, 10000]$ ,  $s \in [-0.001, -0.003, -0.01]$ ,  $L\mu \in [1, 3, 10, 30]$ , and  $L\rho$  logarithmically spaced between  $s$  and 1.0. For the analysis, simulations were filtered such that  $\xi_b > 30$ ,  $\xi_b < L/3$ , and  $\langle T_2 \rangle \mu < 0.5$

Supplementary figure 2: beneficial mutations with fixed effect

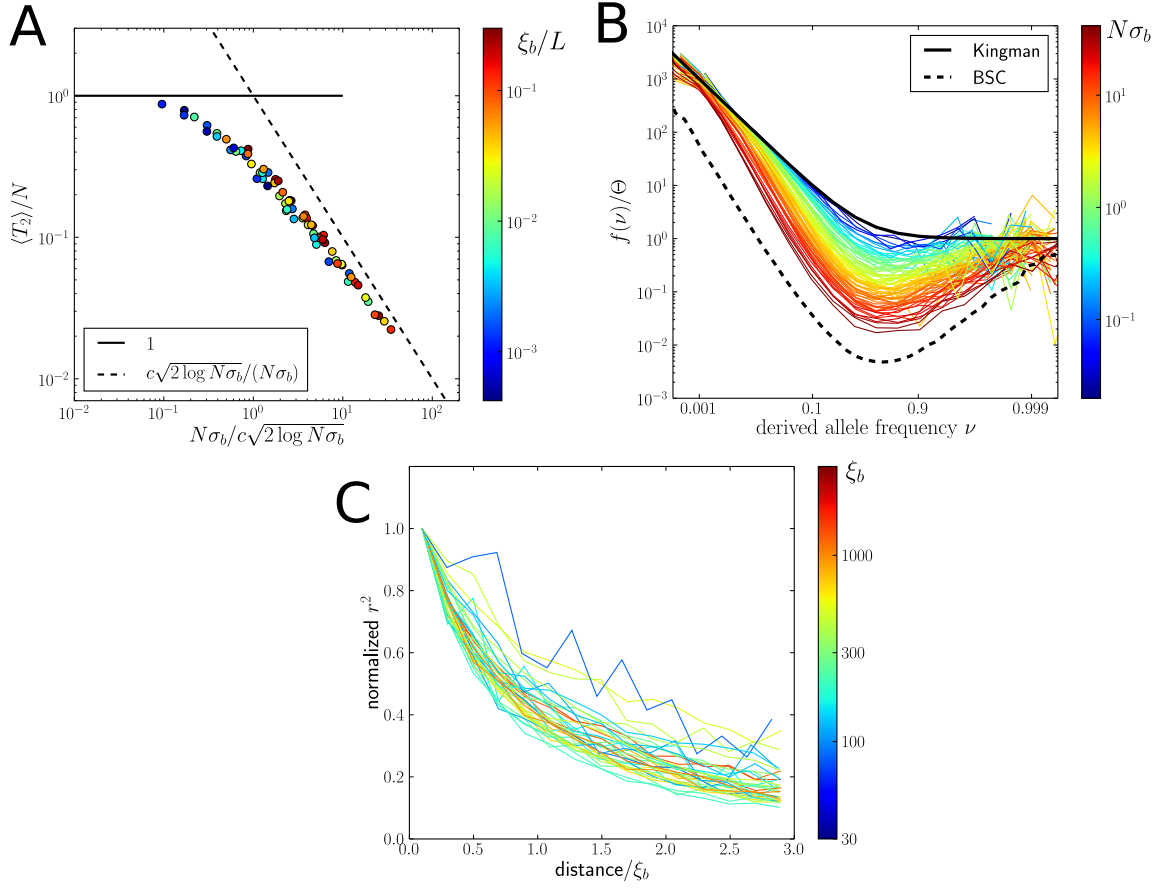


Figure 2 Genetic diversity in populations with frequently sweeping beneficial mutations. Panel A shows the pairwise coalescence time compared to the analytical predictions in the limits of large and small  $N\sigma_b$ . Panel B shows the SFS normalized to  $\Theta = 2N\mu$  (the SFS are obtained from local coalescent trees). Different curves are colored by their respective  $N\sigma_b$  values. The BSC curve serves as a guide to the eye since its proper normalization depends on  $N\sigma_b$ . Panel C shows the decay of LD measured as  $r^2$  and normalized with its value at short distances. The x-axis is rescaled by  $\xi_b$ . The resulting collapse demonstrates that LD extends over distances  $\xi_b$ . In these simulations, mutations are introduced into a random individual whenever a locus becomes monomorphic, analogous to the simulations with constant fitness variance discussed in the main text. However, in this set of simulations, the fitness variance is a fluctuating quantity. The grid of parameters used was  $L \in [3000, 10000]$ ,  $N \in [1000, 3000, 10000]$ ,  $s \in [0.001, 0.003, 0.01]$ , and  $L\rho$  logarithmically spaced between  $s$  and 1.0. For the analysis, simulations were filtered such that  $\xi_b > 30$  and  $\xi_b < L/3$ .

Supplementary figure 3: deleterious and beneficial mutations in an infinite sites model

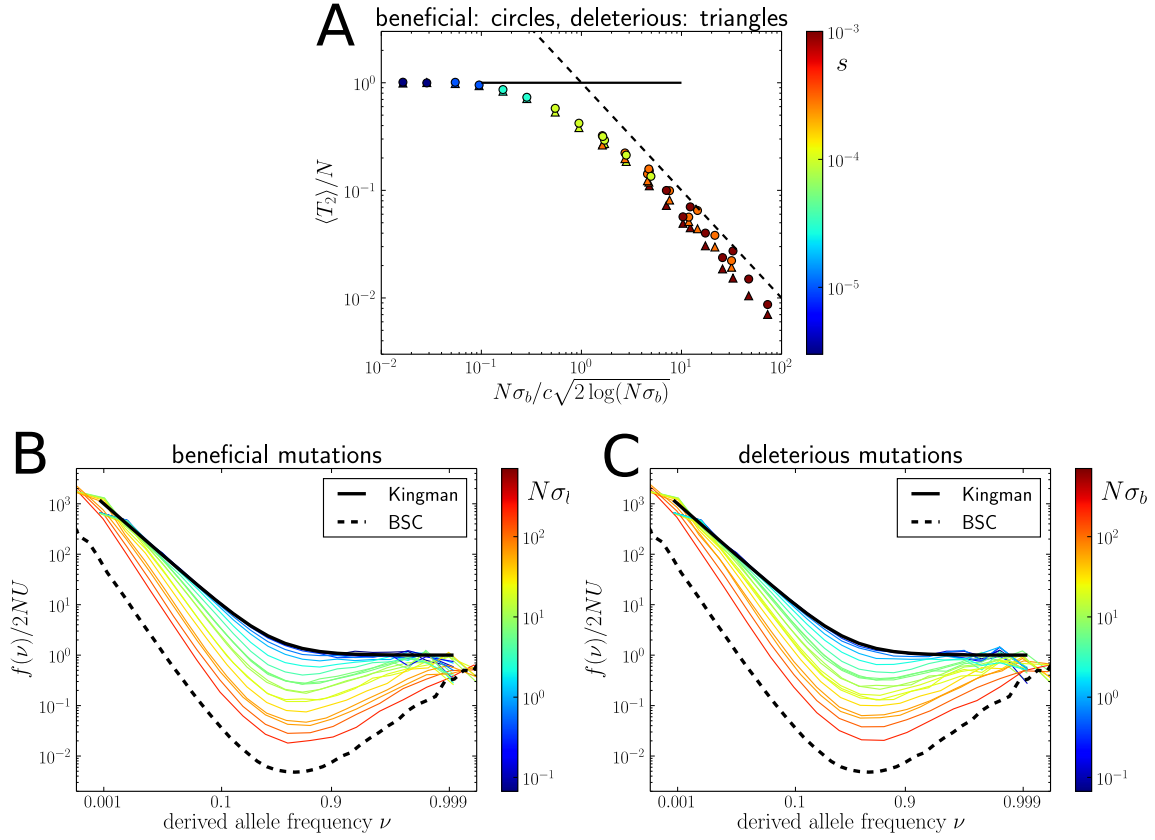


Figure 3 Beneficial and deleterious mutations in a bona fide infinite sites model. Panel A shows the pairwise neutral diversity or coalescence time for simulations with beneficial (circles) and deleterious (triangles) mutations. The color of the symbols indicates the absolute effect size of mutations. Panels B&C show the corresponding SFS for beneficial and deleterious mutations, respectively. The SFS are obtained from histograms of the frequency of neutral polymorphisms and normalized to  $\Theta = 2NU_n$ , where  $U_n$  is the total neutral mutation rate. These results are obtained with a model that assumes chromosomes of length 1 that undergo exactly one crossover per generation. The chromosomes mutate at random places in the interval  $[0, 1]$ . With probability 0.5, mutations are neutral; otherwise they have an effect  $s$  on fitness. We simulate a total mutation rate  $U \in [10, 30, 100]$  with effect sizes  $[3 \times 10^{-5}, 10^{-4}, 3 \times 10^{-3}, 10^{-3}, 3 \times 10^{-3}]$  (positive and negative) for population sizes  $N \in [1000, 3000, 10000]$ . The SFS and the neutral diversity follow the predictions of the analysis presented in the paper. LD was not investigated using this model.